# ON HIGHER ORDER FINITE ELEMENT DISCRETIZATIONS FOR THE INCOMPRESSIBLE NAVIER-STOKES EQUATIONS IN THREE DIMENSIONS

**Volker John**[*]**, Gunar Matthies**[*]**, and Lutz Tobiska**[*]

[*]Otto-von-Guericke-Universität Magdeburg, Institut für Analysis und Numerik,
PSF 4120, 39016 Magdeurg, Germany

**Key words:** Navier-Stokes equations, higher order finite elements, multigrid solvers

**Abstract.** *For solving complex three-dimensional flow problems, many different approaches have been developed. It turns out that both the discretization concept and the solver designed for the discrete problem influences essentially the accuracy and efficiency of the method. The main objective of the paper is to compare lower and higher order finite element discretizations for the accurate and fast solution of the incompressible Navier-Stokes equation in three space dimensions. To this end, a well-defined benchmark problem of a channel flow around an obstacle is used to quantify the gain in accuracy when higher order discretizations are used. The comparison covers also the robust and efficient solution of the discretized algebraic equations.*

## 1 NAVIER-STOKES EQUATION

In this section, we describe the basic concept for solving the incompressible Navier-Stokes equations in a three-dimensional bounded domain $\Omega \subset R^3$,

$$\begin{aligned} -\nu\Delta u + (u\cdot\nabla)u + \nabla p &= f \quad \text{in } \Omega, \\ \nabla\cdot u &= 0 \quad \text{in } \Omega, \\ u &= g \quad \text{on } \partial\Omega, \end{aligned} \tag{1}$$

for the velocity $v$, the pressure $p$, and given data $f$ and $g$, respectively. Let $L^2(\Omega)$, $H^m(\Omega)$, and $H_0^1(\Omega)$ be the usual Lebesgue and Sobolev spaces, and $L_0^2(\Omega)$ be the subspace of all functions $v \in L^2(\Omega)$ with $\int_\Omega v\, dx = 0$. By $(.,.)$ we denote both the scalar product in $L^2(\Omega)$ and in its vector valued variants. Let us assume that $g$ in (1) is the trace of a function (for simplicity again denoted by $g$) from $H^1(\Omega)$, with $\nabla\cdot g = 0$. Using the function spaces $V := H_0^1(\Omega)^3$ and $Q := L_0^2(\Omega)$ the weak formulation of (1) reads as follows:

Find $(u,p) \in (g+V)\times Q$ such that for all $(v,q) \in V\times Q$

$$\nu(\nabla u,\nabla v) + ((u\cdot\nabla)u, v) - (p,\nabla\cdot v) + (q,\nabla\cdot u) = (f,v). \tag{2}$$

It is known, that for $f \in H^{-1}(\Omega)^3$ problem (2) admits at least one solution which is uniquely determined provided that the data are small compared to $\nu$.

Choosing finite element spaces $V_h \approx V$, $Q_h \approx Q$, and a discrete divergence free interpolant $g_h$, we obtain the discrete problem:

Find $(u_h,p_h) \in (g_h+V_h)\times Q_h$ such that for all $(v_h,q_h) \in V_h\times Q_h$

$$\nu(\nabla_h u_h,\nabla_h v_h) + n_h(u_h,u_h,v_h) - (p_h,\nabla_h\cdot v_h) + (q_h,\nabla_h\cdot u_h) = (f,v_h) \tag{3}$$

where the integrals have to be understood in an elementwise manner to allow also non-conforming finite element discretizations. The trilinear form $n_h$ in (3) is defined as

$$n_u(w_h,u_h,v_h) = ((w_h\cdot\nabla_h)u_h, v_h).$$

In the case of dominated convection, which is often true on coarse meshes, a stabilization technique becomes necessary. Then, we use an upwind discretization described in [13] where the amount of stabilization can be controlled by a proper chosen weighting function. In the next section, we introduce the finite element spaces and address the solvability and uniqueness of the discrete problem (3).

The discrete problem (3) corresponds to a nonlinear algebraic system of equations. For the linearization, the following fixed-point iteration will be used:

Given $u_h^{k-1} \in g_h + V_h$, compute $(u_h^k, p_h^k) \in (g_h+V_h)\times Q_h$ such that

$$\nu(\nabla_h u_h^k,\nabla_h v_h) + n_h(u_h^{k-1},u_h^k,v_h) - (p_h^k,\nabla_h\cdot v_h) + (q_h,\nabla_h\cdot u_h^k) = (f,v_h) \tag{4}$$

for all $(v_h,q_h) \in V_h\times Q_h$. Note, that (4) is equivalent to a saddle point problem whose solution will be addressed in Section 3.

## 2 FINITE ELEMENT SPACES

In this section, we describe the finite element spaces which we have used in our numerical tests.

Let $\mathcal{T}_h$ be a decomposition of the domain $\Omega$ either into hexahedra or tetrahedra. The diameter of a cell $K$ is denoted by $h_K$.

In the following, we will consider only those pairs of finite element spaces $V_h, Q_h$, which fulfil the inf-sup or Babuška-Brezzi condition, i.e., there exist a constant $\beta > 0$ independent of the triangulation $\mathcal{T}_h$ such that

$$\inf_{q_h \in Q_h} \sup_{v_h \in V_h} \frac{(\nabla_h \cdot v_h, q_h)}{|v_h|_1 \, \|q_h\|_0} \geq \beta, \tag{5}$$

where $\|\cdot\|_0$ and $|\cdot|_1$ denote the norm in $L^2(\Omega)$ and the seminorm in $H^1(\Omega)^3$, respectively. In case of small data, (5) together with the coerciveness of $(\nabla_h \cdot, \nabla_h \cdot)$ guarantee the unique solvability of the discrete problem (3).

First, we will introduce finite elements on hexahedra. Let $(-1,1)^3$ be the reference cube $\hat{K}$ and $F_K$ the reference transformation from $\hat{K}$ onto the cell $K$. In general, the mapping $F_K$ is trilinear. Let $Q_k(\hat{K})$ and $P_k(\hat{K})$ be the following sets of polynomials on $\hat{K}$

$$Q_k(\hat{K}) := \left\{ \hat{q}(\hat{x}) = \sum_{i,j,l}^{k} a_{ijl} \hat{x}_1^i \hat{x}_2^j \hat{x}_3^l \right\}, \quad P_k(\hat{K}) := \left\{ \hat{p}(\hat{x}) = \sum_{i+j+l \leq k} b_{ijl} \hat{x}_1^i \hat{x}_2^j \hat{x}_3^l \right\}$$

where $\hat{x} = (\hat{x}_1, \hat{x}_2, \hat{x}_3)$. Then, we define

$$Q_k(K) := \left\{ q = \hat{q} \circ F_K^{-1} \ : \ \hat{q} \in Q_k(\hat{K}) \right\}, \quad P_k(K) := \left\{ p = \hat{p} \circ F_K^{-1} \ : \ \hat{p} \in P_k(\hat{K}) \right\}$$

and

$$\begin{aligned} Q_k &:= \left\{ v \in H^1(\Omega) \ : \ v|_K \in Q_k(K) \right\}, \quad k \geq 1, \\ Q_0 &:= \left\{ v \in L^2(\Omega) \ : \ v|_K \in Q_0(K) \right\}, \\ P_k^{disc} &:= \left\{ v \in L^2(\Omega) \ : \ v|_k \in P_k(K) \right\}, \quad k \geq 0. \end{aligned}$$

Furthermore, let $Q_1^{rot}$ be the space of nonconforming, point-value oriented, rotated trilinears defined in [8, 11]. In our numerical tests, we used the following inf-sup stable pairs of finite element spaces:

- $Q_1^{rot}/Q_0$, $Q_2/P_1^{disc}$, $Q_2/Q_1$, $Q_3/P_2^{disc}$.

As usual, the facts that the velocity space is a vector-valued function and the finite element space of the pressure is intersected with $L_0^2(\Omega)$ are not indicated in these notations. Note that we use mapped finite elements which in general do not coincise with the corresponding finite element spaces in which polynomials are defined on the original cell $K$. Indeed, on a general hexahedral cell $K$ the spaces $P_k(K)$ defined above and

$$\tilde{P}_k(K) = \{p(x) = \sum_{i+j+l\le k} b_{ijl} x_1^i x_2^j x_3^l\}$$

are different. The proof that the finite element pairs $Q_2/P_1^{disc}$ and $Q_3/P_2^{disc}$ defined above satisfy an inf-sup condition has been given recently in [7]. Moreover, in [6] it was shown that on a family of successively refined meshes these pairs of elements also preserve the convergence order.

Now, we want to describe the finite elements which we have used on tetrahedra. Let us denote for $k \geq 1$ by $P_k$ the space of continuous, piecewise polynomials of degree less than or equal to $k$, by $P_0$ the space of piecewise constant functions, and by $P_1^{nc}$ the space of nonconforming, piecewise linears which are continuous at the midpoint of each face. The last space was introduced and analysed in [2]. On tetrahedra, we use the two following pairs of finite element spaces:

- $P_1^{nc}/P_0$, $P_2/P_1$.

The case where the domain $\Omega$ has a non-polyhedral boundary, the application of isoparametric elements is useful. In order to obtain an isoparametric reference transformation, all degrees of freedom which belong to a curved faced were move from the plane face onto the real domain boundary. This technique was applied for $Q_2/P_1^{disc}$, $Q_2/Q_1$, $Q_3/P_2^{disc}$ and $P_2/P_1$.

## 3 THE SOLVERS OF THE LINEAR SADDLE POINT PROBLEMS

In each step of the fixed point iteration, one has to solve a linear saddle point problem of the form

$$\mathcal{A}\begin{pmatrix} u \\ p \end{pmatrix} = \begin{pmatrix} A & B \\ C & 0 \end{pmatrix}\begin{pmatrix} u \\ p \end{pmatrix} = \begin{pmatrix} f \\ g \end{pmatrix}. \qquad (6)$$

We will study four types of solvers of (6) which are based on (strongly) coupled multigrid methods.

Two types of solvers use a multigrid method as stand alone solver. The first type is a standard multigrid method which uses on each level of the geometric grid refinement the same discretization. The second type is a modified multigrid method which was introduced in [5]. The construction of this multigrid method is motivated by the observation that multigrid methods are efficient solvers for systems arising from stable lowest order non–conforming discretizations. The top of the multigrid hierarchy consists in the higher order discretization on the finest geometric grid level, see Figure 1. The next coarser level is defined by a stable non–conforming discretization of lowest order on the same level. All other coarser levels consists of stable lowest order non–conforming discretizations on the coarser geometric grid levels.

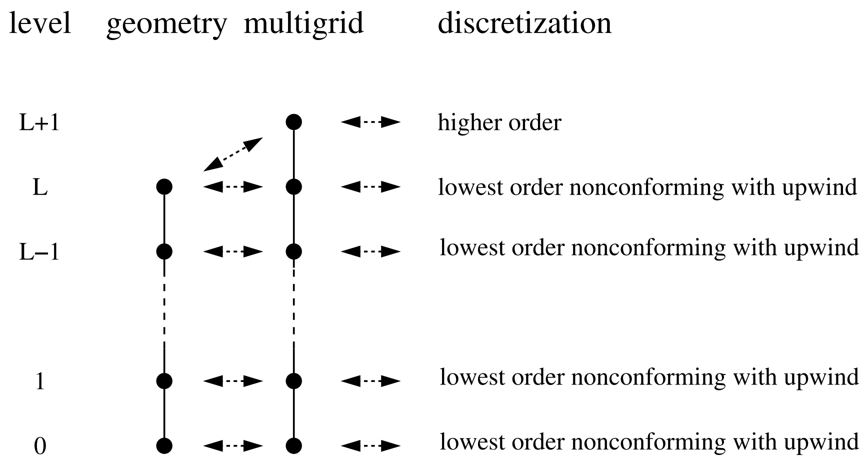


Figure 1: The modified multigrid approach for higher order discretizations.

The multigrid methods have been already described, in the two–dimensional case, in [5] such that we like to give here only short explanations.

We use Vanka–type smoothers which are block Gauss–Seidel methods. Each block consists of a number of degrees of freedom which are used to define a local system of equations. One smoothing step consists of a loop over all blocks, solving the local systems and updating the degrees of freedom in a Gauss–Seidel manner. Of course, there are several possibilities to the define the blocks of degrees of freedom. It was proposed in [5] to take for discretizations with discontinuous pressure approximation all degrees of freedom which are connected to one mesh cell. This defines the so–called mesh cell oriented Vanka smoother. For discretizations with continuous pressure approximation, each block contains only one pressure degree of freedom and all velocity degrees of freedom which are connected with this pressure degree of freedom in the matrix $C$. We call this smoother pressure node oriented Vanka smoother. The local matrix for a block is defined by the intersection of the rows and the columns of the global matrix which are connected to the degrees of freedom contained in the block. This type of Vanka smoother is called full Vanka smoother in [5]. The local systems are solved by Gaussian elemination.

The prolongation in the multigrid methods is done by a grid transfer operator defined by Schieweck [12], see also [5] for a description. This operator allows the transfer between almost arbitrary finite element spaces. Such a transfer is needed in the modified multigrid method between the multigrid levels $L$ and $L+1$. The convergence of the modified multigrid W–cycle with this transfer operator and smoothers of Braess-Sarazin type [1] has been proven for the Stokes equations in [4].

In the third and fourth type of solver, we use the standard multigrid method and the modified multigrid method as preconditioner in the flexible GMRES (FGMRES) method by Saad [9].

## 4 NUMERICAL STUDIES

### 4.1 The problem

We studied the discretizations and solvers presented in the previous sections at the benchmark problem "Flow around a cylinder" defined in [10]. The computational domain is presented in Figure 2. Inflow boundary conditions of the form

$$\mathbf{u} = \begin{pmatrix} \dfrac{7.2y(0.41-y)z(0.41-z)}{0.41^4} \\ 0 \\ 0 \end{pmatrix}$$

are prescribed. For the outflow, either the same boundary conditions or outflow boundary conditions were allowed to prescribe. We will give our choice for the individual studies below. On all other boundaries, homogeneous Dirichlet boundary conditions are applied.

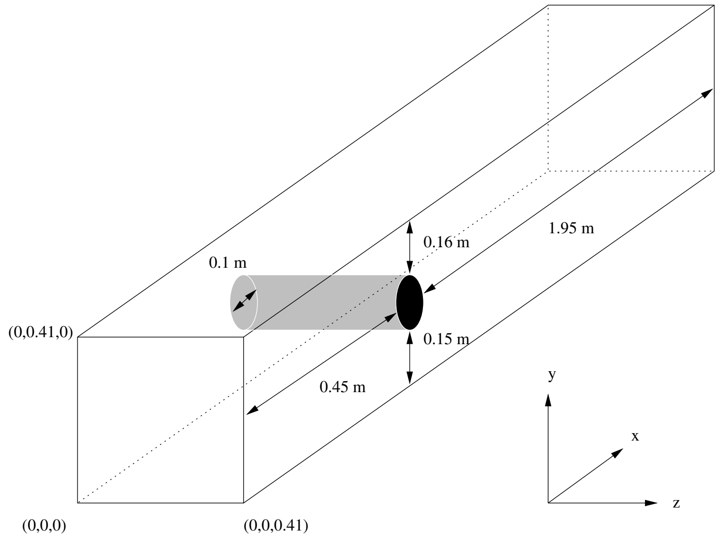


Figure 2: Channel with cylinder.

The benchmark coefficients are the drag and the lift coefficient at the cylinder. In [10], these values are defined by surface integrals on the cylinder. As pointed out in [5], these surface integrals can be transformed into volume integrals whose integrands vanish outside the first layer on mesh cells around the cylinder. We used this volume integral technique to compute both coefficients.

### 4.2 A study of the accuracy of the discretizations

First, we study the accuracy of the computed drag coefficients $c_d$ and lift coefficients $c_l$ obtained with the different pairs of finite element spaces and discretizations introduced in Section 2. The results are presented in Figure 3 and 4. In [10], the following reference intervals are defined: $c_{d,ref} \in [6.05, 6.25]$, $c_{l,ref} \in [8e-3, 1e-2]$. These intervals are depicted with dotted lines in these figures.

The results with respect to the drag coefficient show that the Samarskij upwind discretization of the lowest order non–conforming finite element spaces give by far the most inaccurate results. Even with several million degrees of freedom, the computed drag coefficients are not in the reference interval ($P_1^{nc}/P_0$) or just at the boundary of the reference interval ($Q_1^{rot}/Q^0$). In contrast, the computed drag coefficients with the higher order discretizations are in the reference interval often already on the coarsest level. A closer look of these drag coefficients, Figure 3 bottom, leads to the conjecture $c_{d,ref} \in [6.18, 6.19]$. Comparing the isoparametric and the non–isoparametric boundary approximations shows that the computed drag coefficient with the isoparametric boundary approximation is always closer to the expected reference interval. Thus, higher order isoparametric finite element discretizations give the most accurate drag coefficients in our study.

The main observations for the lift coefficient are the same as for the drag coefficient. Higher order discretizations give by far more accurate results than lowest order non–conforming discretizations with upwind stabilization. It can be seen in Figure 4 that the result obtained with the $P_1^{nc}/P_0$ finite element is still completely wrong for approximately 7 million degrees of freedom. Among the higher order discretizations, the lift coefficient computed with the $P_2/P_1$ finite element on the tetrahedral grid does not reach the benchmark interval with about 500 000 degrees of freedom. But there is a strong tendency towards the reference interval. A closer look of the most accurate results, Figure 4 bottom, suggests that $c_{l,ref} \in [9.3e-3, 9.5e-3]$. The higher accuracy of the isoparametric boundary approximation is not clear from the computed lift coefficients since they cannot be compared to an exact value. But the study presented in [5] of the two dimensional Navier–Stokes equations and the results obtained for the drag coefficient suggest that more accurate results with isoparametric boundary approximation can be expected also here.

### 4.3 A study of the solvers

A second study deals with the behaviour of the solvers introduced in Section 3. In these tests, we applied outflow or "do–nothing" boundary conditions as studied in [3]. We present one test for a discretization with discontinuous pressure approximation using the mesh cell oriented Vanka smoother and one test for a discretization with continuous pressure approximation where the pressure node oriented Vanka smoother was applied. The multigrid methods were applied with the simplest choices of parameters, i.e. without damping of the smoother, without step length control etc.

The initial guess for the fixed point iteration on the finest level was the interpolation of the solution on the next coarser level. The non–linear iteration was stopped for an Euclidean norm of the residual less than $10^{-10}$. The linear saddle point problems (6) were solved in each step of the fixed point iteration up to a reduction of the Euclidean norm of

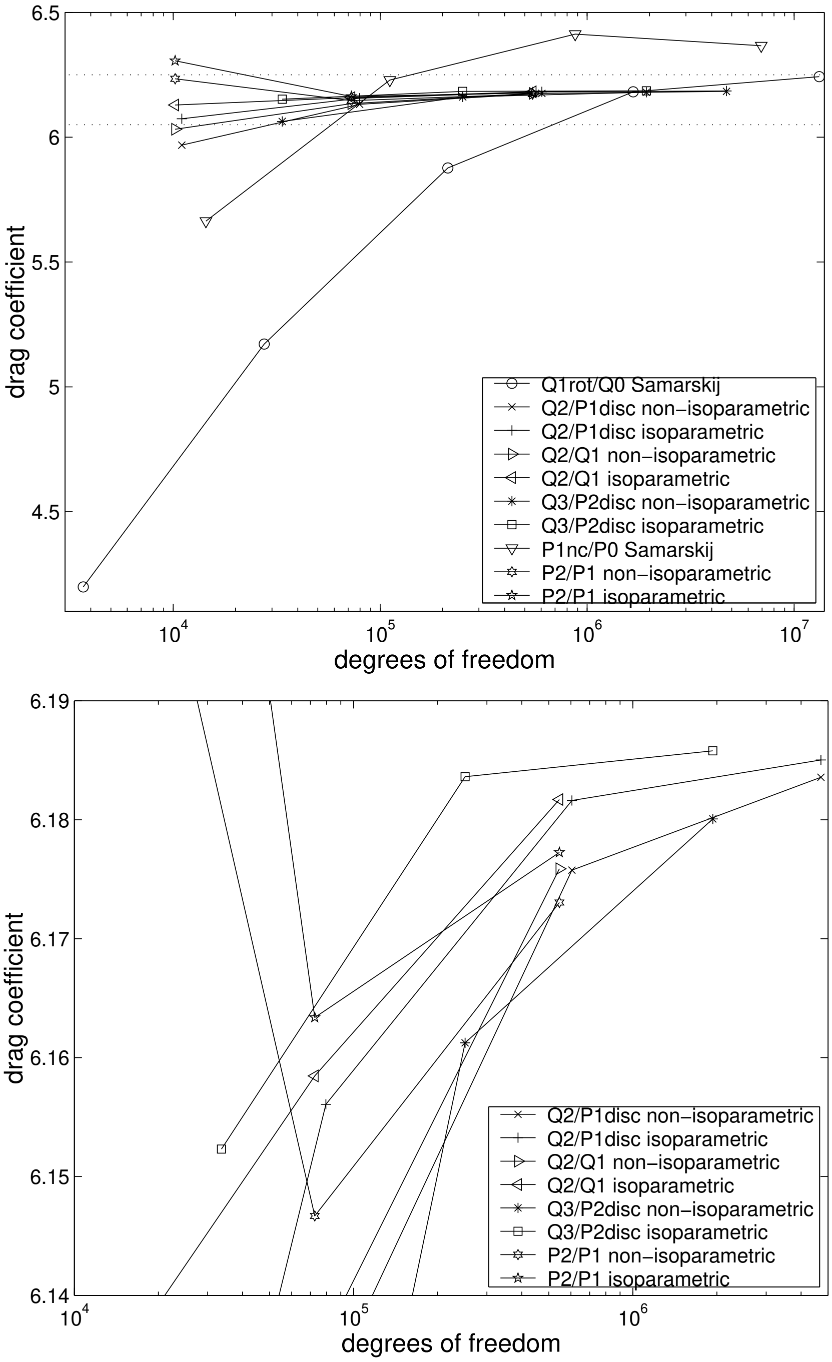


Figure 3: The computed drag coefficients

the residual by the factor 10 or the iteration was stopped after 10 steps. Using a multigrid method as preconditioner, we applied one cycle in each step of the FGMRES iteration. In Tables 1 and 2, the number of fixed point iterations (it) which was necessary to solve

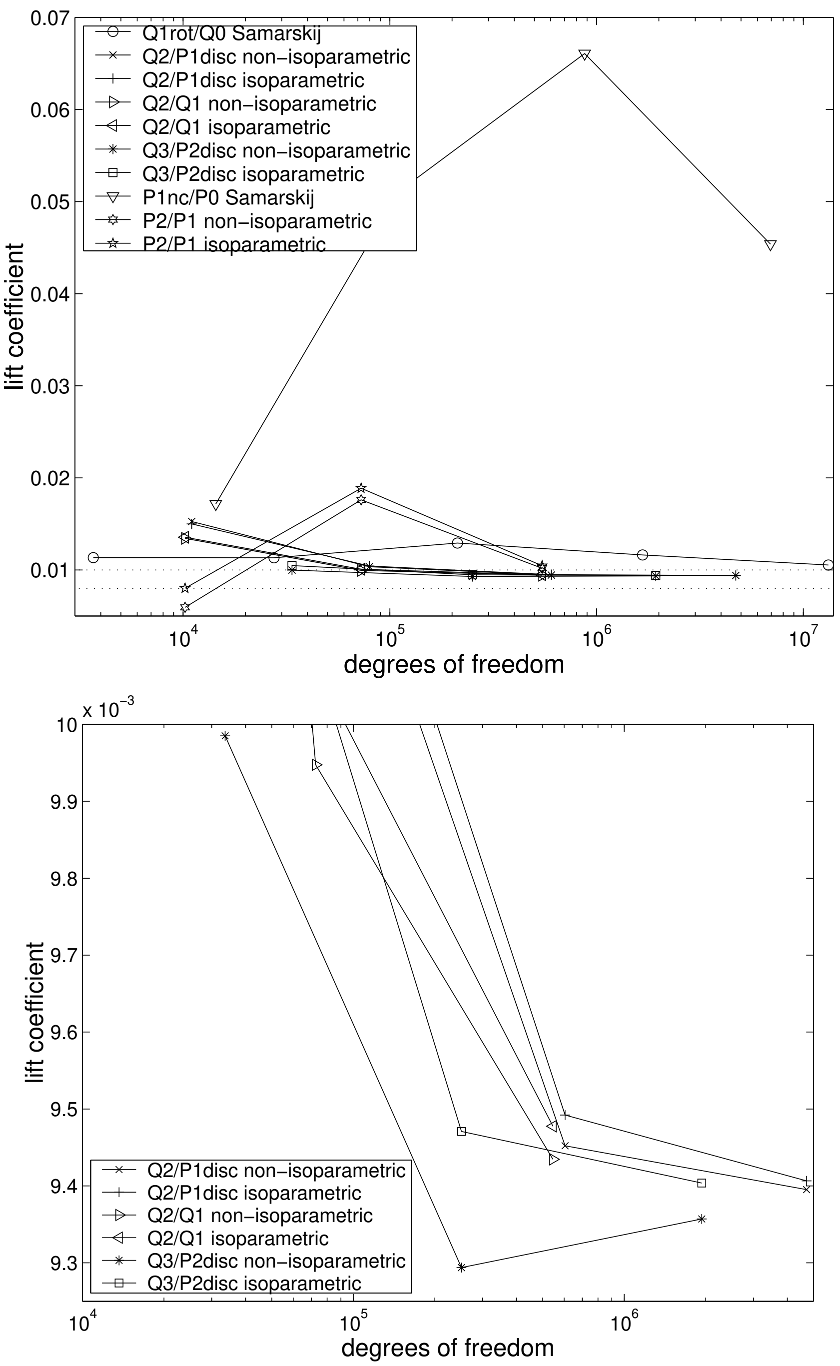


Figure 4: The computed lift coefficients

the Navier–Stokes equations on the given level, the total number of multigrid cycles (cyc) in the fixed point iteration and the computing time are given.

Table 1 presents results obtained for the $Q_2/P_1^{disc}$ finite element discretization on the

| cycle | standard mg | | FGMRES + standard mg | | modified mg | | FGMRES + modified mg | |
|---|---|---|---|---|---|---|---|---|
| | mg cyc. | time | mg cyc. | time | mg cyc. | time | mg cyc. | time |
| $V(1,1)$ | 26 | 19182 | 25 | 18572 | - | div. | 43 | 27982 |
| $V(2,2)$ | 20 | 28772 | 17 | 24672 | 34 | 43628 | 31 | 39851 |
| $V(3,3)$ | 17 | 36335 | 14 | 30319 | 26 | 49789 | 25 | 47950 |
| $V(4,4)$ | 13 | 36848 | 11 | 31302 | 20 | 51048 | 19 | 48516 |
| $F(1,1)$ | 19 | 16778 | 19 | 16941 | 27 | 18239 | 23 | 15584 |
| $F(2,2)$ | 12 | 20129 | 11 | 18599 | 21 | 28004 | 18 | 24029 |
| $F(3,3)$ | 11 | 27172 | 10 | 25141 | 15 | 29793 | 15 | 29875 |
| $F(4,4)$ | 10 | 32598 | 10 | 32711 | 13 | 34435 | 12 | 31783 |
| $W(1,1)$ | 19 | 17418 | 19 | 17426 | 27 | 18379 | 21 | 14345 |
| $W(2,2)$ | 12 | 20656 | 11 | 19209 | 20 | 26820 | 15 | 20150 |
| $W(3,3)$ | 11 | 27752 | 10 | 25617 | 15 | 30021 | 15 | 30040 |
| $W(4,4)$ | 10 | 33231 | 10 | 33355 | 13 | 34642 | 11 | 29304 |

Table 1: Isoparametric $Q_2/P_1^{disc}$ discretization, multigrids with mesh cell oriented Vanka smoother

geometric grid level 3 for 4 711 360 degrees of freedom. It can be seen that the standard multigrid method works well as solver, even better than the modified multigrid method. The modified multigrid method turns out to be the better preconditioner for FGMRES. The FGMRES solver with the $W(1,1)$ modified multigrid preconditioner leads to the fastest solution time. In most tests, the solution time could be reduced by using the multigrid methods as preconditioner instead as solver. But altogether, the differences in the behaviour of these four solvers are not large enough in this test to state clear preferences.

The situation is much different for the $P_2/P_1$ finite element discretization, see Table 2. For this discretization, we present results on the geometric level 1 with 72 600 degrees of freedom. Here, the standard multigrid approach failed. We think that damping the smoother might improve the situation somewhat. But even without damping, we were able to solve the problems with the modified multigrid method. The use of both multigrid approaches as preconditioner in FGMRES enhances the efficiency and the robustness of the solver considerably. For the most types of cycles, the FGMRES with the standard multigrid method converges. The computing times of the FGMRES with the modified multigrid method as preconditioner are much smaller than with the modified multigrid method used as solver. In this test, the clearly best solver is FGMRES with the modified multigrid method as preconditioner.

We observed that the solution of the systems arising in discretizations with continuous pressure approximation is much harder than for the discretizations with discontinuous pressure approximation. The computing times for the $Q_2/P_1^{disc}$ discretization with 4 711 360 degrees of freedom are similar to the computing times for the $P_2/P_1$ discretization

| cycle | standard mg mg cyc. | standard mg time | FGMRES + standard mg mg cyc. | FGMRES + standard mg time | modified mg mg cyc. | modified mg time | FGMRES + modified mg mg cyc. | FGMRES + modified mg time |
|---|---|---|---|---|---|---|---|---|
| $V(1,1)$ | no conv. | - | no conv. | - | 60/600 | 38840 | 29/290 | 19049 |
| $V(2,2)$ | div. | - | 12/116 | 26915 | 52/520 | 66972 | 12/112 | 14623 |
| $V(3,3)$ | div. | - | 12/100 | 31622 | 27/270 | 52136 | 12/89 | 17298 |
| $V(4,4)$ | div. | - | 12/80 | 31697 | 29/290 | 74522 | 12/71 | 18381 |
| $F(1,1)$ | no conv. | - | no conv. | - | 33/330 | 21962 | 14/140 | 9655 |
| $F(2,2)$ | div. | - | 12/116 | 27044 | 38/380 | 49849 | 13/110 | 14832 |
| $F(3,3)$ | div. | - | 12/100 | 31750 | 28/280 | 55138 | 12/92 | 18381 |
| $F(4,4)$ | div. | - | 12/80 | 31829 | 29/290 | 75763 | 12/72 | 19077 |
| $W(1,1)$ | no conv. | - | no conv. | - | 33/330 | 21961 | 14/140 | 9656 |
| $W(2,2)$ | div. | - | 12/116 | 26959 | 38/380 | 49863 | 13/110 | 14833 |
| $W(3,3)$ | div. | - | 12/100 | 31667 | 28/280 | 55092 | 12/92 | 18374 |
| $W(4,4)$ | div. | - | 12/80 | 31681 | 29/290 | 75750 | 12/72 | 19084 |

Table 2: Isoparametric $P_2/P_1$ discretization, multigrids with pressure node oriented Vanka smoother, (div. - divergent, no conv. - iteration stagnates away from the solution)

and 72 600 degrees of freedom.

### 4.4 Conclusions

The most important conclusions of our study are as follows:

- Drag and lift coefficients in the 3D benchmark problem defined in [10] could be computed most accuarately with higher order isoparametric finite element discretizations.
- The FGMRES method with the modified multigrid method has been proven as an efficient and robust solver for the arising linear saddle point problems.

**Acknowledgement:** The second author was partially supported by DFG grant FOR 301.

## REFERENCES

[1] D. Braess and R. Sarazin. An efficient smoother for the Stokes problem. *Applied Numer. Math.*, 23(1):3 – 19, 1997.

[2] M. Crouzeix and P.-A. Raviart. Conforming and nonconforming finite element methods for solving the stationary Stokes equations I. *R.A.I.R.O. Analyse Numérique*, 7:33–76, 1973.

[3] J.G. Heywood, R. Rannacher, and S. Turek. Artificial boundaries and flux and pressure conditions for the incompressible Navier-Stokes equations. *Int. J. Numer. Methods Fluids*, 22(5):325–352, 1996.

[4] V. John, P. Knobloch, G. Matthies, and L. Tobiska. Non-nested multi-level solvers for finite element discretizations of mixed problems. Preprint, Fakultät für Mathematik, Otto-von-Guericke-Universität Magdeburg, 2001.

[5] V. John and G. Matthies. Higher order finite element discretizations in a benchmark problem for incompressible flows. to appear in Int. J. Num. Meth. Fluids, 2001.

[6] G. Matthies. Mapped finite elements on hexahedra. necessary and sufficient conditions for optimal interpolation errors. Preprint 3, Otto-von-Guericke Universität Magdeburg, Fakultät für Mathematik, 2001.

[7] G. Matthies and L. Tobiska. The inf-sup condition for the mapped $Q_k - P_{k-1}^{disc}$ element in arbitrary space dimensions. Preprint 01-02, Fakultät für Mathematik, Otto-von-Guericke-Universität Magdeburg, 2001.

[8] R. Rannacher and S. Turek. Simple nonconforming quadrilateral Stokes element. *Numer. Meth. Part. Diff. Equ.*, 8:97 – 111, 1992.

[9] Y. Saad. A flexible inner-outer preconditioned GMRES algorithm. *SIAM J. Sci. Comput.*, 14(2):461–469, 1993.

[10] M. Schäfer and S. Turek. The benchmark problem "Flow around a cylinder". In E.H. Hirschel, editor, *Flow Simulation with High–Performance Computers II*, volume 52 of *Notes on Numerical Fluid Mechanics*, pages 547 – 566. Vieweg, 1996.

[11] F. Schieweck. *Parallele Lösung der stationären inkompressiblen Navier–Stokes Gleichungen.* Otto-von-Guericke Universität Magdeburg, Fakultät für Mathematik, 1997. Habilitation.

[12] F. Schieweck. Analysis of post-processing for nonconforming finite element solutions. Preprint 00-25, Fakultät für Mathematik, Otto-von-Guericke-Universität Magdeburg, 2000.

[13] F. Schieweck and L. Tobiska. An optimal order error estimate for an upwind discretization of the Navier–Stokes equations. *Num. Meth. Part. Diff. Equ.*, 12:407 – 421, 1996.